

A Method for Measuring Optical Properties of Semitransparent Materials at High Temperatures

V.H. Myers,* A. Ono,† and D.P. DeWitt‡

School of Mechanical Engineering, Purdue University, West Lafayette, Indiana

A method is described for determination of the optical properties, refractive index, and extinction coefficient of nonscattering semitransparent materials at high temperatures from measurements of two independent radiative properties. The sample holder confined within a thin-walled, direct electrically heated tube accommodates a slab-shaped sample and provides the necessary (three) isothermal targets. The radiative and optical properties of fused quartz and sapphire at 1000°C and 0.6-13 μm are reported and compared favorably with the available data in the literature. The major source of error is veiling glare (scattering of unwanted radiance) originating from the sample holder; within the semitransparent region, accuracies of better than 10% for the optical properties are possible.

Nomenclature

a	= absorption coefficient, m^{-1}
d	= thickness of slab sample, m
L	= radiance, $\text{W} \cdot \text{m}^{-2} \cdot \mu\text{m}^{-1} \cdot \text{sr}^{-1}$
n	= refractive index
r	= radiance ratio
R	= Fresnel reflectivity
T	= temperature, °C or K
T_λ	= internal spectral transmissivity
ϵ	= emissivity
κ	= extinction coefficient
λ	= wavelength
ρ	= external reflectivity
τ	= external transmissivity

Subscripts

b	= blackbody conditions
bs	= cavity-hole radiance target
h	= blackbody radiance reference target
o	= vacuum condition
r	= room temperature reference condition
s	= sample radiance target, sample ratio
vg	= veiling glare
z	= radiometric zero reference target
λ	= spectral modifier for properties

Superscripts

$()'$	= corrected radiance ratio values
--------	-----------------------------------

Introduction

THE analysis of radiative heat transfer from high-temperature opaque materials requires knowledge of the surface radiative properties, emissivity, absorptivity, or reflectivity. For semitransparent materials, effects due to volumetric absorption and emission, temperature gradients within the material, and (system) geometry may be important and thus the radiative properties are no longer adequate to

describe the transfer process. Rather, analysis is accomplished through use of the radiative equation of transfer that requires knowledge of the optical properties, the refraction index n , and the extinction coefficient κ . While all radiometric-type measurements at high temperature are difficult to make, determination of the optical properties is especially tedious since at least two radiative properties must be independently measured. As a consequence, there is a dearth of optical property data in the literature and methods for their determination are necessarily complicated.

Only a few methods have been reported in the literature for the determination of both optical properties. The method of Stierwalt¹ is based upon three radiance observations: that of a freely radiating nonscattering slab sample, a blackbody reference, and a slab sample positioned in front of a blackbody. The observations can be used to directly determine emissivity and transmissivity from which the optical properties can be calculated knowing the slab thickness. Stierwalt used a heated copper block into which each of the above configurations was independently inserted, measured, and then removed. Gryvnak and Burch² developed a method in which the transmissivity of two different thicknesses of the same material were measured and related to the optical properties. The two cylindrical samples with flat parallel faces were mounted in a furnace in such a manner that they could be translated into and out of the optical path of the detection system. Both of these methods have shortcomings in the form of inconvenience (complicated positioning mechanisms). The latter method has the severe requirement on sample preparation that the two samples have identical composition but different thicknesses.

Several methods have been developed for direct determination of one optical property; by application of a limiting assumption or the use of known literature data, the second optical property can be inferred. Dvurechenskii et al.³ have made emissivity measurements on various grades and thicknesses of fused quartz and utilized literature data on the room temperature refractive index to determine the extinction coefficient. Their technique, the most recent of all work, requires a rapid-scan spectrometer (ms) for sensing spectral radiance of a sample that is rapidly removed from the heating furnace. Morichev et al.⁴ related the measured emissivity of thin quartz samples directly to the absorption coefficient (ignoring multiple reflections). Vanyushin and Petrov⁵ and Edwards⁶ made transmissivity measurements of two thicknesses of low-reflectivity materials (sapphire and fused quartz, respectively)

Presented as Paper 83-1500 at the AIAA 18th Thermophysics Conference, Montreal, Canada, June 1-3, 1983. Received July 23, 1983; revision received May 1, 1985. Copyright © American Institute of Aeronautics and Astronautics, Inc., 1983. All rights reserved.

*Graduate Research Assistant, (presently with IBM, Poughkeepsie, NY).

†Visiting Scholar (from Japan Laboratory for Metrology).

‡Professor. Member AIAA.

to obtain the absorption coefficient. Oppenheim and Even⁷ measured the transmissivity of plane slab samples and utilized room temperature data from the literature for the refractive index to determine the absorption coefficient of sapphire. Wray and Neu,⁸ using a minimum deviation technique, measured the angle of refraction of a collimated radiation beam passing through the prism-shaped sample to determine the refractive index. These methods are cumbersome to implement, often limited in their applicability to special sample geometries and spectral ranges, and beset with systematic errors such as nonisothermal conditions among the radiance targets.

To overcome the shortcomings and inconveniences of previous methods, a new method was sought that would require only one sample and minimal experimental inconveniences or loss of accuracy in making the various radiance observations (sample, references, etc.). Furthermore, the new method would utilize several features of an emissometer apparatus developed during our previous work on the measurement of the high-temperature emissivity of conducting and nonconducting opaque materials.⁹⁻¹¹ Under the constraints of the existing apparatus, the objectives of the present work have been to design a sample holder that accommodates a simple sample geometry and provides appropriate radiance targets, allowing the optical properties to be directly related to the measurable radiative properties; to evaluate the sample holder arrangement; and to demonstrate the accuracy of the method by comparison of measurements on fused quartz and sapphire with optical properties reported in the literature.

The Measurement Method

Sample Heating Tube Configuration

Figure 1 shows a front and side view of the sample heating arrangement. The slab-shaped sample is mounted within the equalizing block which is radiatively coupled to the direct electrically heated tube. The block (20 mm length by 10 mm diameter) is fabricated from high-purity nickel and has four cavities or holes serving as radiance targets. The cavity diameters are 1.6 mm and the three lower targets are within 9 mm of each other. A sample up to 3 mm thick can be accommodated and is held in good thermal contact with the block by a stainless steel set screw. The equalizing block is positioned at the midpoint of the heating tube (René, 292 mm length by 10.5 mm diameter) on an aluminum oxide disk supported by stainless steel pins to prevent passage of electric current through the block. The tube holes are slightly oversized (2.0 mm) to simplify alignment. A water-cooled graphite block (not shown) with two long cylindrical cavities is positioned behind the heating tube. One cavity provides a uniform near-room temperature background for the through-hole and

the other, viewed directly by the Emissometer, serves as the radiometer zero reference target.

Radiance observations are made of three high-temperature isothermal targets following the principle employed by Stierwalt¹: the slab sample positioned in front of the blackbody (cavity-hole), the freely radiating sample (through-hole), and the blackbody reference. A fourth observation is made of the graphite water-cooled cavity for the radiometric zero signal. While only one high-temperature blackbody reference is required for the observation process, the second one provides the means to check the temperature uniformity of the block.

The major assumptions made in the model for formulating target radiances are: isothermal conditions between the radiance targets; planar, nonscattering (specular) slab sample; surroundings of the heating tube are isothermal and black; and the surrounding medium has unity refractive index. The cavity-hole (*bs*) radiance L_{bs} consists of sample emission plus blackbody radiance transmitted through the sample,

$$L_{bs} = \epsilon_{\lambda} L_{\lambda,b}(\lambda, T_s) + \tau_{\lambda} L_{\lambda,b}(\lambda, T_s) \quad (1)$$

where ϵ_{λ} and τ_{λ} are sample emissivity and transmissivity, respectively, $L_{\lambda,b}$ the spectral blackbody radiance, and T_s the temperature of the sample and blackbodies. Since the temperature of the heating tube surroundings (water-cooled vacuum enclosure) is nearly room temperature, there is a negligible contribution to L_{bs} from reflected irradiance. The through-hole (*s*) radiance L_s consists of sample emission only,

$$L_s = \epsilon_{\lambda} L_{\lambda,b}(\lambda, T_s) \quad (2)$$

since radiance from the surroundings at room temperature transmitted through or reflected into the direction of viewing will be negligible. The blackbody reference (*h*) radiance L_h is prescribed by the Planck distribution,

$$L_h = L_{\lambda,b}(\lambda, T_s) \quad (3)$$

The radiometric zero reference (*z*) radiance L_z is obtained by viewing the water-cooled graphite cavity at near-room temperature. This term accounts for any dc or modulated offset in the radiation detection system.

Property Relations

The radiance observations made on the three high-temperature and one zero reference targets are combined to form two ratios. The sample ratio r_s is

$$r_s = (L_s - L_z) / (L_h - L_z) \quad (4)$$

while blackbody-sample ratio value r_{bs} has the form

$$r_{bs} = (L_{bs} - L_z) / (L_h - L_z) \quad (5)$$

Substituting Eqs. (1-4) into Eqs. (5) and (6), and using the radiative balance relation

$$\epsilon_{\lambda} + \tau_{\lambda} + \rho_{\lambda} = 1$$

the ratios become

$$r_s = \epsilon_{\lambda}, \quad r_{bs} = 1 - \rho_{\lambda} \quad (6,7)$$

The external radiative properties, ϵ_{λ} and ρ_{λ} , include the effects of interreflections between the two plane, specular surfaces of the nonscattering sample and are thus dependent upon the Fresnel, or surface, reflectivity R_{λ} and the internal transmissivity T_{λ} . These two sets of radiative properties are related by two nonlinear algebraic equations of the form

$$\epsilon_{\lambda} = \frac{(1 - T_{\lambda})(1 - R_{\lambda})}{1 - T_{\lambda}R_{\lambda}} \quad (8)$$

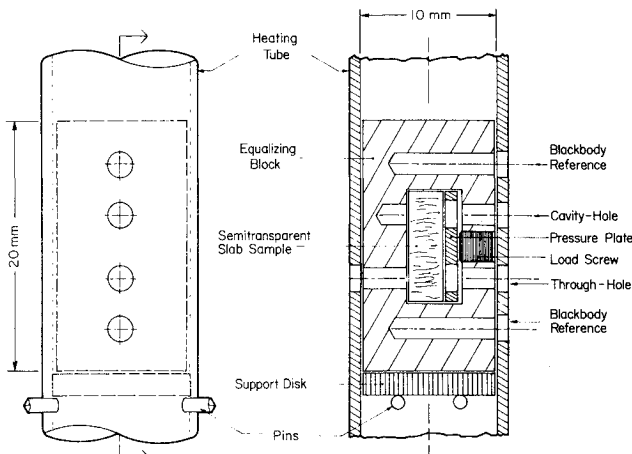


Fig. 1 Sample and sample holder mounted within the heating tube.

and

$$\tau_\lambda = \frac{T_\lambda(1 - R_\lambda)^2}{1 - (T_\lambda R_\lambda)^2} \quad (9)$$

which must be solved iteratively. For simplicity in solving the equations by the Newton-Raphson method, τ_λ instead of ρ_λ is related to the internal radiative properties.

These radiative properties may now be related to the optical properties. For radiation propagating through a nonscattering planar medium of thickness d ,

$$a_\lambda = -\ln(T_\lambda)/d \quad (10)$$

where a_λ is the spectral absorption coefficient. The extinction coefficient κ_λ is related to the absorption coefficient by

$$\kappa_\lambda = a_\lambda \lambda_o / 4\pi \quad (11)$$

where λ_o is the spectral radiance wavelength in a vacuum. The refractive index n_λ is determined from the Fresnel reflectivity relation for normal incidence conditions,

$$R_\lambda = \frac{(n_\lambda - 1)^2 + \kappa_\lambda^2}{(n_\lambda + 1)^2 + \kappa_\lambda^2} \quad (12)$$

This equation is quadratic in n_λ and may be solved from knowledge of R_λ and κ_λ values.

The Measurement Procedure

The experimental apparatus utilized for realization of the new method consists of the Emissometer, the Multiproperty Apparatus, and the digital data acquisition system (DDAS). The details of these components and their application to the measurement of high temperature emissivities of opaque conducting and non-conducting materials have been previously published.⁹⁻¹¹ Some of the important features added to the experimental apparatus since this work include: an Infrared Associates liquid-nitrogen-cooled trivalent metal detector (Hg-Cd-Te, 1.1-4.6 μm , 0.0645 cm^2 active area, 3.9 μm peak response), a United Detector silicon photodiode (PIN 5-D, 0.7-1.0 μm , 0.051 cm^2 active area, 0.85 μm peak response), a LiF prism, and a sapphire planoconvex lens (0.5-5.0 μm) at the exit slit to the monochromator. These additions represent improvements in the near-infrared response (0.6-4.6 μm) of the Emissometer. Use of the DDAS program developed for the Emissometer has been modified for the measurement of semitransparent materials.

With the sample mounted in the equalizing block (initially heavily oxidized and then lightly scrapped and blown clean with compressed air), the heating tube is clamped between the two water-cooled electrodes within the enclosure of the multiproperty apparatus. The Emissometer is then carefully positioned in front of the enclosure viewing window to ensure near-normal viewing of the radiance targets. The enclosure is maintained at 1 torr to prevent oxidation of the sample without destroying the nickel holder oxide layer. When the heating tube is brought to the desired temperature level, the observation process for the sample ratio r_s is initiated. The solenoid-controlled mirror of the Emissometer is adjusted to sequentially view the through-hole, blackbody reference, and zero reference (only three positions are possible). The initial wavelength is set and the computer program directs the Emissometer to make radiance observations of the zero reference, blackbody reference, and through-hole targets and then calculates r_s as well as the standard deviations of the observed signals. Next, the blackbody-sample ratio r_{bs} is obtained. The solenoid-controlled mirror is adjusted to sequentially view the cavity hole, blackbody reference, and zero reference and radiance observations are automatically made. Thus, two radiative properties, emissivity and reflectivity, are obtained from two independent sets of measurements. The next wavelength is selected and the procedure is repeated. The

optical properties (and their uncertainties) are subsequently calculated from the measured radiative properties using Eqs. (10-12).

Performance Evaluation

Studies were undertaken to evaluate the quality of the reference blackbody cavities, the isothermal condition of the equalizing block and sample, and the effect of veiling glare (transfer optics scattering).

Blackbody Cavities

The reference blackbodies are cylindrical cavities with a depth-to-diameter ratio of 5.3, having conical bottoms with apex angle of 120 deg. Their surfaces are left roughened by the drilling process and then blackened by oxidation of the nickel surfaces. Following the method developed by Ono,¹² the quality of the cavities are estimated to be better than 0.998.

The temperatures of the two reference blackbodies and the cavity hole without a sample (now also a blackbody in this configuration) were measured with a radiation thermometer. The maximum variation was no more than 0.5°C, which is the resolution of the thermometer. The spectral radiance temperature of the René heating tube outer surface at the midlength was observed to be uniformly 10°C higher over the section containing the equalizing block than beyond (higher or lower) this section. The elevated temperature condition is due to the higher volumetric heating in the central section (five holes in the tube reduce the cross-sectional area for current flow) and to the decreased radiative losses from the inside walls of the tube (the equalizing block has increased the thermal resistance). It is apparent that this condition has not adversely affected the temperature distribution within the equalizing block.

Isothermal Conditions

The temperature uniformity of the sample was inferred from emissivity measurements on an opaque, polished (but with slight diffuse appearance) aluminum oxide sample. Radiances were observed from the cavity-hole (*bs*) and through-hole (*s*) targets (see Fig. 1) and, since the sample was opaque, the radiances were due only to sample emission. Based upon 10 observations on each target location, the emissivity values were nearly identical at 0.967 (within 0.005). In the vicinity of the through-hole, both sides of the sample view the cooler enclosure surroundings, while only one side is so exposed at the cavity-hole location. Despite this difference in thermal boundary conditions, the sample temperature uniformity must be very good and related systematic errors are negligible.

From previous measurements by another method,¹⁰ the sample emissivity was known to have a lower value of 0.91. The higher value cannot be a consequence of temperature nonuniformity, but rather is due to radiance from the lateral surface of the hole walls being reflected off the slightly diffuse sample into the Emissometer field of view. This effect, nearly 0.06 emissivity units, will be dependent upon the sample characteristics—emissivity (or reflectivity) magnitude and degree of diffuseness.

Further evidence on the importance of this effect was obtained from emissivity measurements on a second aluminum oxide sample with a roughened, diffuse surface. To increase the lateral wall influence, the sample was mounted slightly nonnormal to the viewing axis, permitting specular reflections to be included in the field of view. This arrangement yielded identical emissivity values for both targets (*bs* and *s*) of 0.998 ± 0.004 , indicating that the behavior of these sample targets is practically the same as the blackbody references (*h*).

From these studies, it can be concluded that the isothermal condition of the sample and equalizing block (and its reference blackbodies) is very good, probably within 0.6°C. The observations on the opaque aluminum oxide samples indicate that reflected radiance from the hole lateral surfaces can cause a

systematically high error in emissivity (or radiance measurements). With a semitransparent sample the effect due to reflection of wall irradiance can also be present; in addition, scattering within the bulk of the sample could give rise to unwanted radiance within the Emissometer field of view.

Veiling Glare

The term veiling glare is applied to the presence of unwanted components in the target radiance and gives rise to significant, but systematic, errors in the determination of the radiative and optical properties of the semitransparent materials being studied. The effect of veiling glare on the method can be evaluated using features of the sample holder.

The veiling glare is defined as the ratio of through-hole radiance L_s to blackbody radiance L_h . For the transparent region of the sample, the veiling glare ratio can be defined as

$$r_{vg} = (L_s - L_z) / (L_h - L_z) \quad (13)$$

With r_{vg} known, the corrected radiance ratios of Eqs. (4) and (5) in the semitransparent and opaque regions will be

$$r_s' = r_s - r_{vg}, \quad r_{bs}' = r_{bs} - r_{vg} \quad (14,15)$$

That is, the effect of veiling glare is to cause a systematic positive error on the calculated ratios, a lower estimate for the refractive index, and a high estimate for the extinction coefficient.

Veiling glare levels of the through-hole without a sample present were minimal (typically, 0.0027) and thus the veiling glare is believed to be due primarily to scattering of high-temperature radiance from the equalizing block by the sample itself. The origin of this scattering (surface or volumetric) is unclear as the veiling glare varied between samples and was wavelength dependent in the transparent region for sapphire. The systematic effect in the transparent region is uncertain and thus the optical properties could not be reliably corrected in those regions where r_{vg} varied. The veiling glare reached a constant minimum before the semitransparent region for both materials and r_{vg} was determined by averaging these minimum values for both samples.

Experimental Results

The results for the measured radiative properties and calculated optical properties are presented in Figs. 2-7 for two thicknesses of fused quartz and one thickness of sapphire at 1000°C. Comparison to the literature of and uncertainties in the calculated optical property data are shown.

Optical-Grade Fused Quartz

The emissivity spectra of two optical-grade fused quartz samples (thicknesses 1.54 and 3.20 mm) are shown in Fig. 2 for the spectral range 0.7-13 μm at 1000°C. These samples (supplied by ESCO Products) contain large but unspecified amounts of hydroxyl ion impurities. The major features of the spectra are: near-zero emissivity in the transparent region from the visible to 2.0 μm ; rapidly changing emissivity in the semitransparent region 2.0-4.3 μm , with characteristic hydroxyl ion absorption bands present at 2.2 and 2.7 μm ; and near-unity emissivity in the opaque region from 4.3 μm on, with a sharp minimum at about 9.0 μm due to a reflectivity increase (restrahlen band). Note the thickness effect in the semitransparent region, where the thicker sample exhibits higher emission (this is also dependent upon the relative percentage of hydroxyl ions in the sample). Data from both samples agree very well in the transparent and opaque regions where the radiative properties should be independent of thickness. Nonzero emissivity (0.01) in the transparent region is a consequence of significant veiling glare either from diffuse reflection of irradiance due to surface roughness and/or contamination, or scattering through the sample volume.

Figure 3 presents the normal reflectivity ρ_λ spectra at 0.7-13 μm ; its major characteristics are: uniform values (0.06) in the transparent region; a decrease to the Fresnel reflectivity value as multiple reflections are reduced by absorption; and near-zero reflectivity at 7.0 μm , followed by a sharp maximum representing a restrahlen band at about 9.0 μm . The 2.2 μm absorption band is too weak to be observed in the reflectivity spectra of either sample. A slight thickness effect is observed in the semitransparent region as the thicker sample data are slightly lower. Good agreement is found between the samples in the transparent and opaque regions.

The extinction coefficient κ_λ for the samples of different thicknesses is presented in Fig. 4 from 2.0 to 4.6 μm . Additionally, the upper inset of the figure presents the uncertainty in the extinction coefficient $\Delta\kappa_\lambda$, based upon the propagation

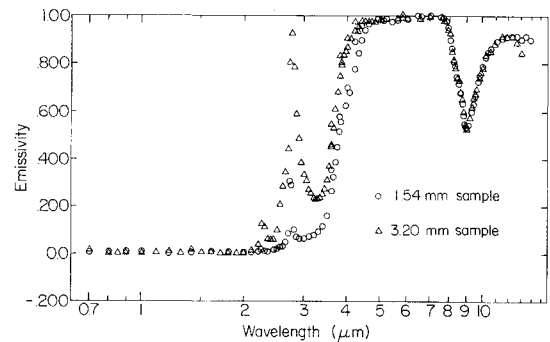


Fig. 2 Spectral, normal emissivity of optical-grade fused quartz at 1000°C.

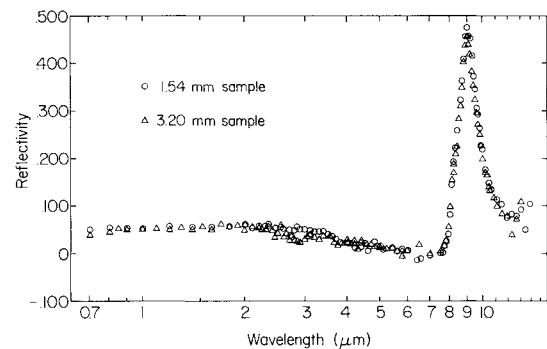


Fig. 3 Spectral, normal reflectivity of optical-grade fused quartz at 1000°C.

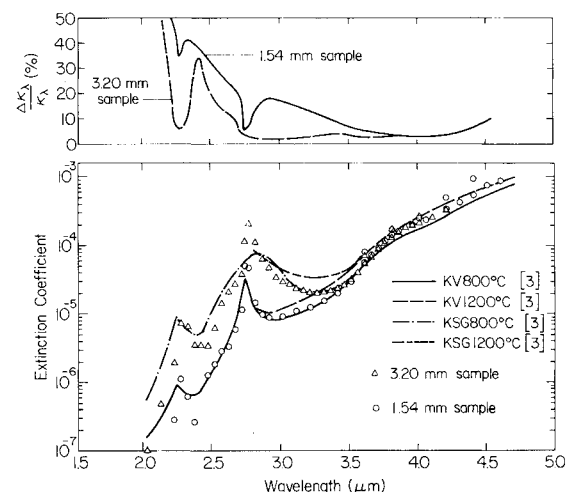


Fig. 4 Spectra extinction coefficient and its relative uncertainty of optical-grade fused quartz at 1000°C.

of uncertainties (precision) of the radiance observations. No data are reported below $2.0\ \mu\text{m}$ because the veiling glare is larger than sample emission or beyond $4.6\ \mu\text{m}$ because the absorption is too high (τ_λ less than 0.01). These spectra are characterized by rapidly increasing values in the semitransparent region with sharp absorption bands at 2.2 and $2.72\ \mu\text{m}$. An unexpected disagreement between the data for the samples is evident in the absorption band region, since κ_λ

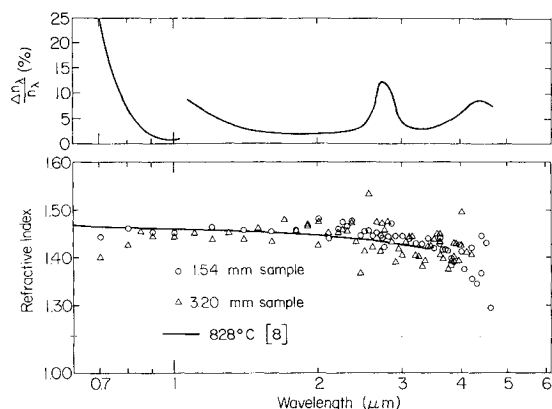


Fig. 5 Spectral refractive index and its relative uncertainty of optical-grade fused quartz at 1000°C .

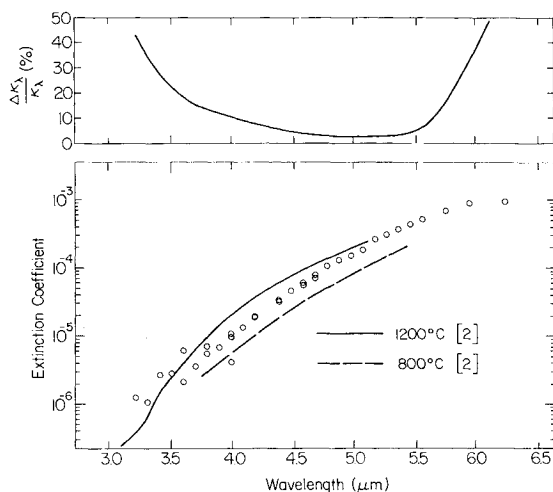


Fig. 6 Spectral extinction coefficient and its relative uncertainty of sapphire at 1000°C .

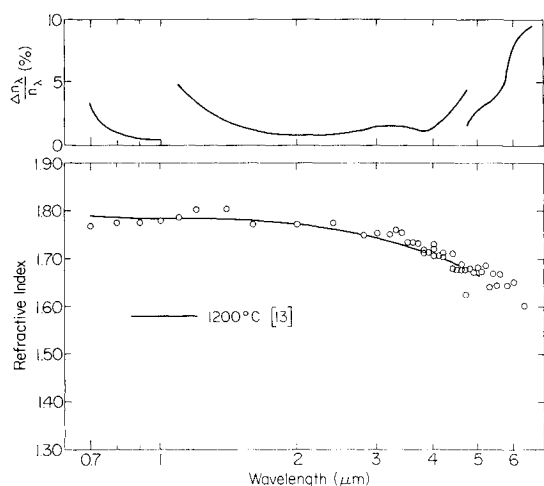


Fig. 7 Spectral refractive index and its relative uncertainty of sapphire at 1000°C .

is an intrinsic property and thus should be independent of the thickness. Note that good agreement is observed beyond $3.3\ \mu\text{m}$, suggesting that the discrepancy in the absorption band region is most likely due to differences in hydroxyl ion concentration. Since the samples were not fabricated from the same stock, there is no reason to expect their composition will be identical. The data compare quite well to values from Dvurechenskii et al.³ for their two grades of fused quartz (KV and KSG), having as high as 15% hydroxyl ion content. The percentage uncertainty values are generally good, decreasing rapidly with longer wavelengths as sample emission increases.

Figure 5 illustrates the refractive index from the visible to $4.6\ \mu\text{m}$ for the two samples of different thicknesses. The spectra is fairly constant until $3.0\ \mu\text{m}$, whereupon the refractive index begins to decrease. Below $2.0\ \mu\text{m}$, the refractive index is weakly dependent on the extinction coefficient and hence, large uncertainties in this region have little influence. These values compare favorably to the data of Wray and Neu⁸ at 828°C . Note that the trend of the data deviates from the literature near the transparent region, especially below $1\ \mu\text{m}$. Uncertainties are large (15%) in the absorption region due to low radiance levels (atmospheric absorption band) and near the opaque region because of low transmittance, but generally are less than 8% outside these regions.

Sapphire

The extinction coefficient spectra for synthetic sapphire ($2.24\ \text{mm}$ thickness, ESCO Products) is shown in Fig. 6. No data are reported below $3.0\ \mu\text{m}$ because sample emission is too low (ϵ_λ less than 0.01). The results are compared to data from Gryvnak and Burch² at 800 and 1200°C . The comparison is favorable from $4\ \mu\text{m}$ to the opaque region; below $4\ \mu\text{m}$, uncertainties are especially noticeable because of low sample emission.

The refractive index spectra of Fig. 7 has uniform values in the transparent region, followed by slightly decreasing values beyond $3.0\ \mu\text{m}$. The results compare favorably to the data by Plass¹³ (room temperature data extrapolated to 1200°C). The data below $1.1\ \mu\text{m}$ deviates somewhat from the literature trend. The correction of data in this region is uncertain because the origin of the veiling glare is not clear. The data are quite smooth and the percentage uncertainty is low even near the opaque region because of the increased reflectivity.

Summary

The features and performance of the new method have been demonstrated. A sample holder was designed that fit compactly inside a heating tube and provided the necessary radiance targets for directly obtaining the radiative properties from which the optical properties could be determined. Evaluation of the sample holder found that the high-temperature targets were within 0.6°C of each other and blackbody reference quality was better than 0.998. Results of fused quartz and sapphire optical properties compared well with data in the literature in the semitransparent region, but varying veiling glare (and its unknown origin) in the transparent region prevented reliable correction of the data in this region.

The method cannot be used to obtain reliable extinction coefficient data in the transparent range because the emission is low (ϵ_λ less than 0.01) and comparable to the veiling glare. Values for the refractive index can be obtained, but with low confidence because of the magnitude and uncertainty in the veiling glare. Veiling glare is less significant in the semitransparent region and appears to assume a uniform value, so that corrections to the data can be made with confidence. The extinction coefficient converged with the literature data in this region and the uncertainties decreased to less than 4%. The refractive index was within 1% of the data in the literature. The uncertainty in the refractive index ranged as high as 15% in some spectral regions for low-reflectivity fused quartz, but generally was less than 8%. Higher-

reflectivity sapphire exhibited lower scatter and uncertainties. Optical property data could not be determined for transmissivities less than 0.01.

The new method is applicable to materials with reflectivities as low as 0.02. Reliable data appear to be obtainable for the semitransparent region where the emissivity and transmissivity are greater than 0.01. The use of thicker samples will increase the measurement capability near the transparent region, but the sample holder is presently limited to samples of 3 mm thickness. Thinner samples can be accommodated, improving the useful range of the method nearer the opaque region. Higher reflectivity materials can be measured, but the veiling glare problem might become even more significant for these materials.

References

- ¹Stierwalt, D.L., "Infrared Spectral Emittance of Optical Materials," *Applied Optics*, Vol. 5, No. 12, 1966, pp. 1911-1915.
- ²Gryvnak, D.A. and Burch, D.E., "Optical and Infrared Properties of Al_2O_3 at Elevated Temperatures," *Journal of the Optical Society of America*, Vol. 55, No. 6, 1965, pp. 625-629.
- ³Dvurechenskii, A.V., Petrov, V.A., and Reznik, V. Yu., "Spectral Emittance of Silica Glasses at High Temperatures," *High Temperatures—High Pressures*, Vol. 11, 1979, pp. 423-428.
- ⁴Morichev, I.E., Onokhov, A.P., and Savinov, V.P., "Laser Breakdown and Temperature Dependence of Absorption in Quartz," *Soviet Physics—Technical Physics*, Vol. 23, No. 10, 1978, pp. 1254-1255.

⁵Vanyushin, A.V. and Petrov, V.A., "Measurement of the Spectral Absorption Coefficient of Ruby and Leucosapphire at High Temperatures," *High Temperatures—High Pressures*, Vol. 8, 1976, pp. 551-556.

⁶Edwards, O.J., "Optical Absorption Coefficients of Fused Silica in the Wavelength Range 0.17 to 3.5 Microns from Room Temperature to 980 C," NASA TN D-3257, 1966, pp. 1-23.

⁷Oppenheim, U.P. and Even, U., "Infrared Properties of Sapphire at Elevated Temperatures," *Journal of the Optical Society of America*, Vol. 52, No. 9, 1962, pp. 1078-1079.

⁸Wray, J.H. and Neu, J.T., "Refractive Index as a Function of Temperature," *Journal of the Optical Society of America*, Vol. 59, No. 6, 1969, pp. 774-776.

⁹DeWitt, D.P., Taylor, R.E., and Riddle, T.K., "High Temperature Computer Controlled Emissometer for Spectral and Total Measurements on Conducting and Non-conducting Materials," *Proceedings of 7th Symposium on Thermophysical Properties*, ASME, New York, 1977, pp. 256-264.

¹⁰Johnson, P.E., DeWitt, D.P., and Taylor, R.E., "Method for Measuring High Temperature Spectral Emissivity of Nonconducting Materials," *AIAA Journal*, Vol. 19, Jan. 1981, pp. 113-120.

¹¹Taylor, R.E., "A Description of the Thermophysical Properties Research Laboratory," Thermophysical Properties Research Laboratory Rept. 181, Feb. 1979.

¹²Ono, A., "Calculation of the Directional Emissivities of Cavities by the Monte Carlo Method," *Journal of the Optical Society of America*, Vol. 70, No. 5, 1980, pp. 547-554.

¹³Plass, G.N., "Temperature Dependence of the Mie Scattering and Absorption Cross Section for Aluminum Oxide," *Applied Optics*, Vol. 4, No. 12, 1965, pp. 1616-1619.

From the AIAA Progress in Astronautics and Aeronautics Series...

FUNDAMENTALS OF SOLID-PROPELLANT COMBUSTION — v. 90

*Edited by Kenneth K. Kuo, The Pennsylvania State University
and
Martin Summerfield, Princeton Combustion Research Laboratories, Inc.*

In this volume distinguished researchers treat the diverse technical disciplines of solid-propellant combustion in fifteen chapters. Each chapter presents a survey of previous work, detailed theoretical formulations and experimental methods, and experimental and theoretical results, and then interprets technological gaps and research directions. The chapters cover rocket propellants and combustion characteristics; chemistry ignition and combustion of ammonium perchlorate-based propellants; thermal behavior of RDX and HMX; chemistry of nitrate ester and nitramine propellants; solid-propellant ignition theories and experiments; flame spreading and overall ignition transient; steady-state burning of homogeneous propellants and steady-state burning of composite propellants under zero cross-flow situations; experimental observations of combustion instability; theoretical analysis of combustion instability and smokeless propellants.

For years to come, this authoritative and compendious work will be an indispensable tool for combustion scientists, chemists, and chemical engineers concerned with modern propellants, as well as for applied physicists. Its thorough coverage provides necessary background for advanced students.

Published in 1984, 891 pp., 6 × 9 illus. (some color plates), \$60 Mem., \$85 List; ISBN 0-915928-84-1

TO ORDER WRITE: Publications Order Dept., AIAA, 1633 Broadway, New York, N.Y. 10019